

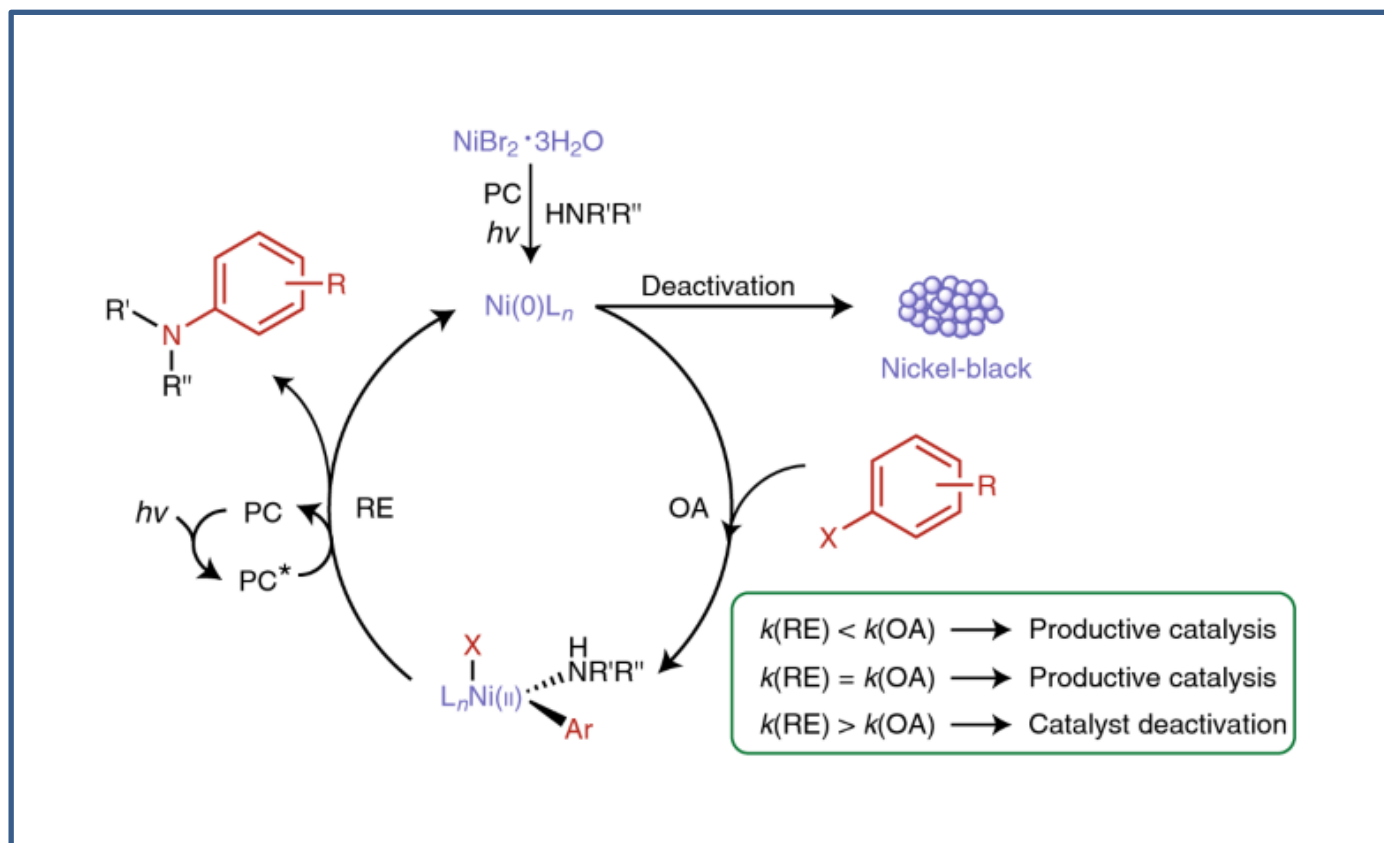


Published in final form as:

Gisbertz, S., Reischauer, S., & Pieber, B. (2020). Overcoming limitations in dual photoredox/nickel catalyzed C–N cross-couplings due to catalyst deactivation. *Nature Catalysis*. doi:10.1038/s41929-020-0473-6

## Overcoming limitations in dual photoredox/nickel catalyzed C–N cross-couplings due to catalyst deactivation

Sebastian Gisbertz, Susanne Reischauer, Bartholomäus Pieber



## ARTICLE

# Overcoming Limitations in Dual Photoredox/Nickel-catalysed C–N Cross-Couplings due to Catalyst

## Deactivation

Sebastian Gisbertz,<sup>1,2</sup> Susanne Reischauer<sup>1,2</sup> & Bartholomäus Pieber<sup>1\*</sup>

<sup>1</sup>*Department of Biomolecular Systems, Max-Planck-Institute of Colloids and Interfaces, Am Mühlenberg 1, 14476 Potsdam, Germany*

<sup>2</sup>*Department of Chemistry and Biochemistry, Freie Universität Berlin, Arnimallee 22, 14195 Berlin, Germany*

*\*Corresponding author*

*Email: bartholomaeus.pieber@mpikg.mpg.de*

### Abstract

Dual photoredox/nickel catalysed C–N cross-couplings suffer from low yields for electron-rich aryl halides. The formation of catalytically inactive nickel-black is responsible for this limitation and causes severe reproducibility issues. Here we demonstrate that catalyst deactivation can be avoided by using a carbon nitride photocatalyst. The broad absorption of the heterogeneous photocatalyst enables a wavelength dependent control of the rate of reductive elimination to prevent nickel-black formation during the coupling of cyclic, secondary amines and aryl halides. A second approach, that is applicable to a broader set of electron-rich aryl halides, is to run the reactions at high concentrations to increase the rate of oxidative addition. Less nucleophilic, primary amines can be coupled with electron-rich aryl halides by stabilizing low-valent nickel intermediates with a suitable additive. The developed protocols enable reproducible, selective C–N cross-couplings of electron-rich aryl bromides and can be also applied for electron-poor aryl chlorides.

## MAIN

The palladium-catalysed formation of carbon–nitrogen bonds (Buchwald-Hartwig) ranks among the most widely applied reactions in synthetic chemistry.<sup>1</sup> Nickel is an attractive alternative to palladium due to its higher abundance, but the requirement of air-sensitive Ni(0) complexes, sophisticated ligands, as well as strong reductants, and bases for C–N bond formations have hampered its use.<sup>2-4</sup> Air-stable nickel pre-catalysts have been developed, but still strong alkoxide bases and complex ligands are needed (Figure 1, a).<sup>5-9</sup> In combination with electrochemistry, ligated Ni(II) salts catalyse the C–N cross-coupling under mild conditions (Figure 1, b).<sup>10,11</sup> Ligand-free Ni(II) salts were used together with UV light (365 nm),<sup>12</sup> or visible light photocatalysis *via* photoredox (PRC),<sup>13-17</sup> or energy transfer (EnT)<sup>18,19</sup> processes (Figure 1, c). Although synthetically attractive, electro- and photochemically mediated, nickel-catalysed C–N couplings are limited to electron-poor aryl halides. Aryl halides that do not contain electron withdrawing groups are usually either unreactive,<sup>15</sup> or give low yields,<sup>11,12,16,17,19</sup> and only a few examples with a good isolated yield are reported (for a detailed analysis, see Supplementary Figure 1-7).<sup>13</sup>

Electro- and photochemically mediated methods rely on the initial reduction of the Ni(II) catalyst to a low valent (Ni<sup>0</sup> or Ni<sup>I</sup>) species, followed by oxidative addition that is slow for electron-rich aryl halides.<sup>11,20</sup> This bottleneck potentially leads to the accumulation of nickel(0) species that aggregate, resulting in catalyst deactivation. In the electrochemically driven, nickel-catalysed aryl amination, nickel-black deposition was observed on the cathode and could be avoided by using Ni(bpy)<sub>3</sub>Br<sub>2</sub> (bpy = 2,2'-bipyridine) instead of a 1:1 mixture of NiBr<sub>2</sub>·glyme and dtbbpy (4,4'-di-tert-butyl-2,2'-bipyridine), thereby expanding the scope to a few electron-rich heteroaryl halides.<sup>11</sup> Stabilizing bipyridine ligands are unsuitable for light-mediated, nickel-catalysed C–N cross-couplings,<sup>12-17</sup> but catalyst deactivation or nickel-black formation was not reported. It is, however, well known that Ni(II) salts – in presence of amines

as sacrificial electron donors (SED) – can be used intentionally for the photochemical preparation of Ni(0) nanoparticles (Figure 1, d).<sup>21-23</sup>

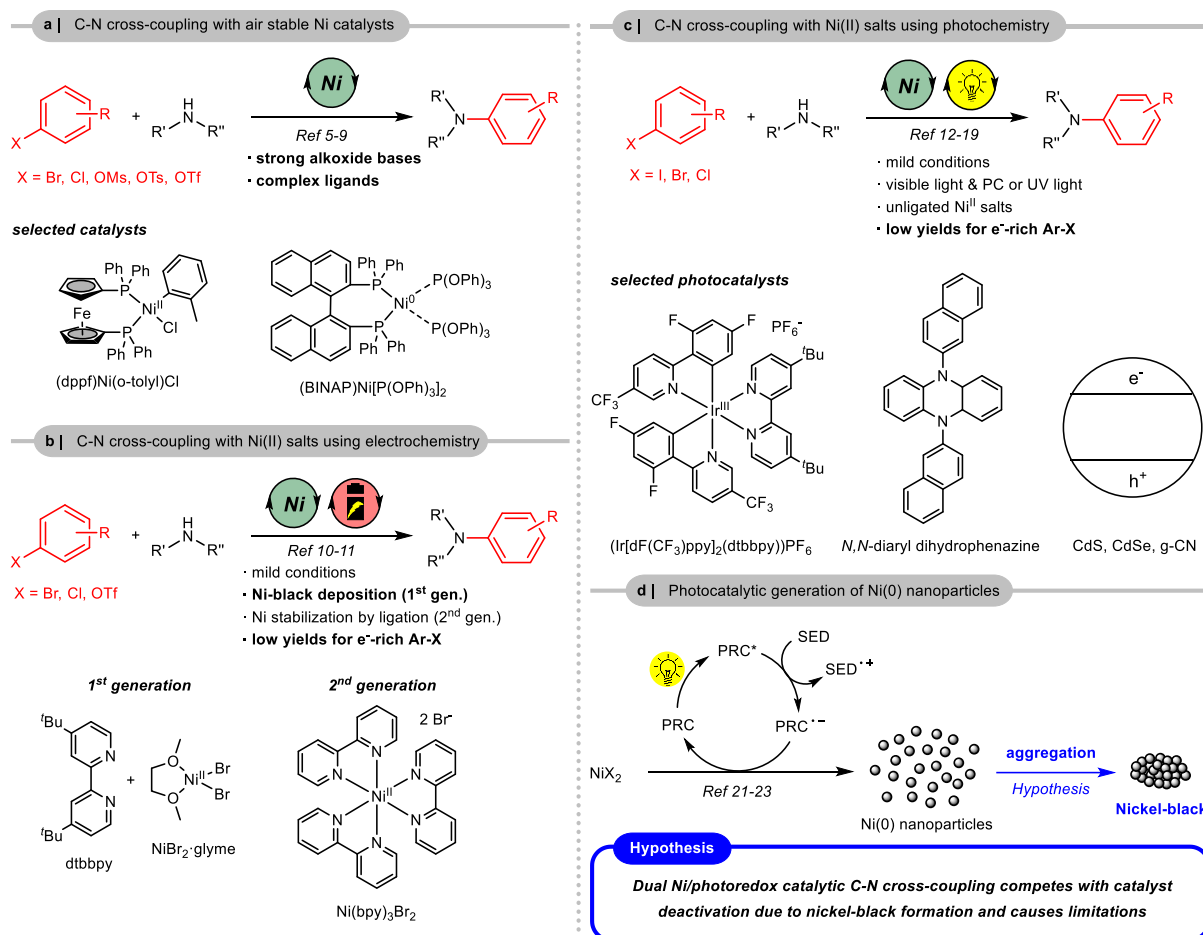


**Figure 1 | Nickel catalysed C–N cross-coupling reactions.** **a**, air stable Ni precatalysts require strong bases and sophisticated ligands. **b**, electrochemically enabled, Ni-catalysed aminations and; **c**, photochemically driven, Ni-catalysed aminations are limited to electron-poor aryl halides. **d**, photocatalytic reduction of Ni(II) salts is used for nanoparticle formation and potentially leads to nickel-black formation in catalysis. dppf = 1,1'-bis(diphenylphosphanyl) ferrocene. BINAP = 2,2'-bis(diphenylphosphino)-1,1'-binaphthyl. dtbbpy = 4,4'-di-tert-butyl-2,2'-bipyridine. glyme = 1,2-dimethoxyethane. bpy = 2,2'-bipyridine. ppy = 2-phenylpyridine. g-CN = graphitic carbon nitride. PRC = photoredox catalyst. SED = sacrificial electron donor.

Here, we show that catalyst deactivation *via* nickel-black formation is responsible for the low yields when electron-rich aryl bromides are used in dual photoredox/nickel catalysed C–N cross-couplings. Deposition of the catalytically inactive, low-valent nickel species further deactivates a heterogeneous photocatalyst, hampering its recyclability. We demonstrate that

nickel-black formation can be avoided by decelerating the light-mediated reductive elimination, enhancing the oxidative addition, or stabilizing low-valent nickel intermediates. The resulting protocols enable selective and reproducible couplings of amines with electron-poor, -neutral, and -rich aryl halides, and allow for recycling of the heterogeneous photocatalyst.

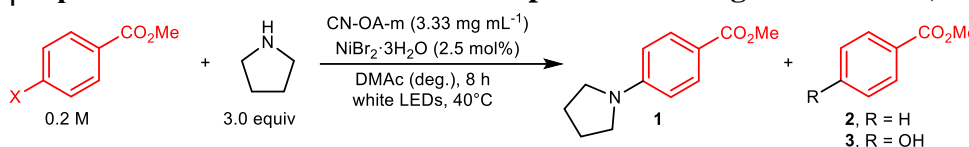
## Results

### Initial optimization studies

Our investigations started by optimizing the dual nickel/photoredox catalysed amination of methyl 4-bromobenzoate with pyrrolidine using the carbon nitride CN-OA-m as photocatalyst (Table 1; for details see Supplementary Note 1). This heterogeneous material has a broader optical absorption in the visible region compared to most other known CN materials and can be easily prepared on gram scale *via* co-condensation of urea and oxamide followed by post-calcination in a molten salt (see Supplementary Figure 8).<sup>24-26</sup> Nearly quantitative formation of the desired alkyl aryl amine (**1**) was obtained within 8 h when CN-OA-m (3.33 mg mL<sup>-1</sup>), NiBr<sub>2</sub>·3H<sub>2</sub>O (2.5 mol%) and three equivalents of the amine were used without any additional base in dimethylacetamide (DMAc) as solvent (Table 1, Entry 1-2). Bulky secondary amines such as *N*-*tert*-butylisopropylamine and 2,2,6,6-tetramethylpiperidine do not couple with aryl halides and can be used as a base if only 1.5 equivalents of pyrrolidine are used (see Supplementary Note 2). The reaction was easily scaled up by increasing the reaction time, affording **1** on a gram scale within 14 hours (see Supplementary Note 3). It was recently shown that such reactions can be efficiently carried out on even larger scales using continuous flow chemistry.<sup>27</sup> Aside from aryl bromides, aryl iodides coupled with similar efficiency and selectivity (Entry 3). The optimized protocol further enabled C–N couplings using aryl

chlorides and aryl triflates, but these reactions did not go to completion (Entry 4-5). Control studies in the absence of CN-OA-m, NiBr<sub>2</sub>·3H<sub>2</sub>O and light did not result in the formation of the desired product, and the presence of oxygen significantly decreased the reaction rate (Entry 6-9).

**Table 1 | Optimized conditions and control experiments using white LEDs (RGB)<sup>[a]</sup>**



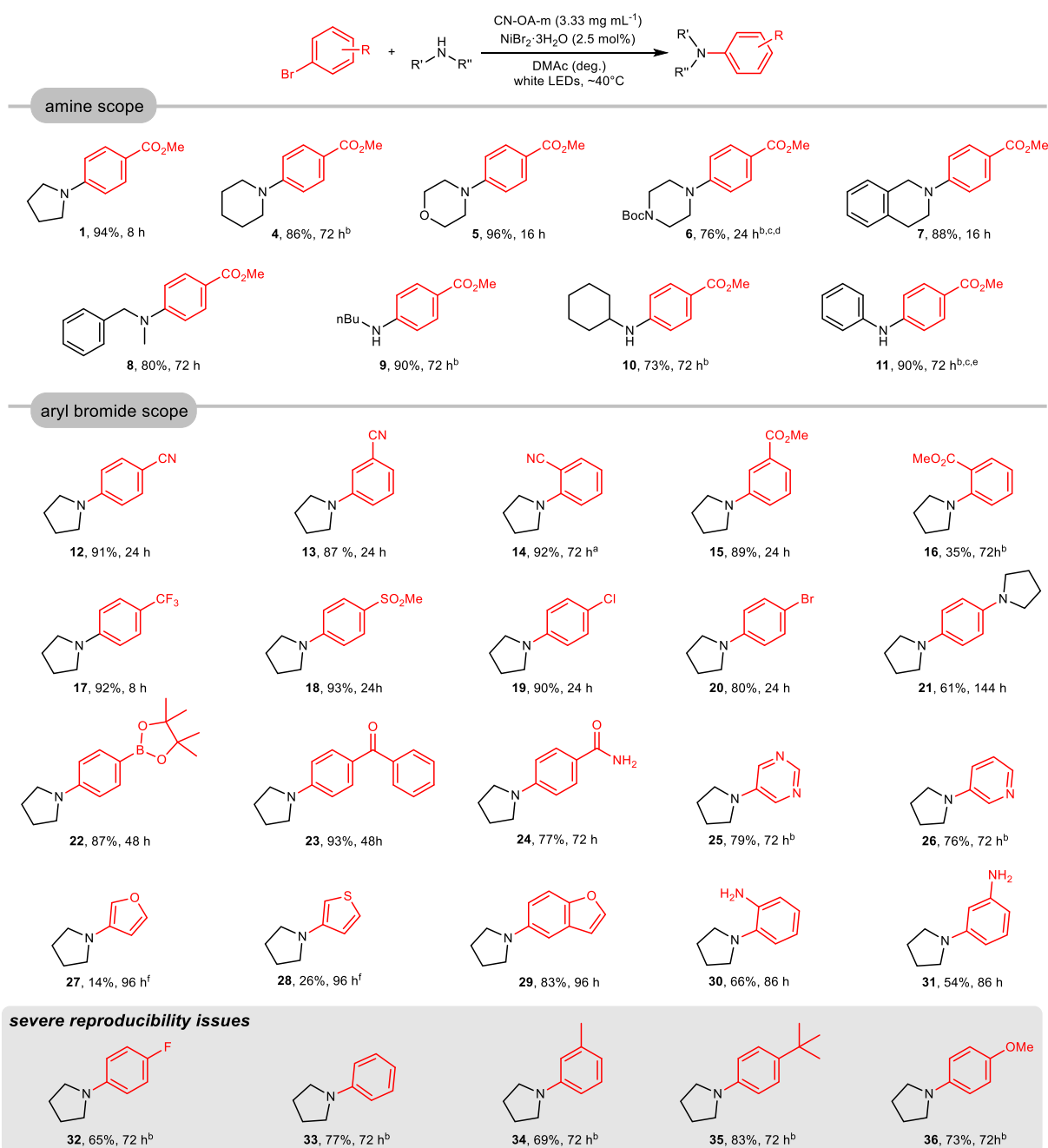
Entry	X	Conditions	Conversion [%] <sup>b</sup>	1 [%] <sup>c</sup>	2 [%] <sup>c</sup>	3 [%] <sup>c</sup>
1	Br	as shown	quant.	98	2	n.d.
2	Br	1.66 mg mL <sup>-1</sup> CN-OA-m	quant.	96	2	1
3	I	as shown	quant.	99	1	n.d.
4	Cl	168 h	76	72	4	n.d.
5	OTf	72 h	75	67	5	2
6	Br	no CN-OA-m	5	n.d.	2	1
7	Br	no NiBr <sub>2</sub> ·3H <sub>2</sub> O	5	n.d.	n.d.	n.d.
8	Br	no light	<1	n.d.	n.d.	n.d.
9	Br	no degassing	10	10	n.d.	n.d.

<sup>a</sup>Reaction conditions: methyl 4-bromobenzoate (1.2 mmol), pyrrolidine (3.6 mmol), NiBr<sub>2</sub>·3H<sub>2</sub>O (2.5 mol%), CN-OA-m (20 mg), DMAc (anhydrous, 6 mL), white LEDs (RGB) at 40 °C for 8 h. <sup>b</sup>Conversion aryl halide determined by <sup>1</sup>H-NMR using 1,3,5-trimethoxybenzene as internal standard. <sup>c</sup>NMR yields were determined by <sup>1</sup>H-NMR using 1,3,5-trimethoxybenzene as internal standard. DMAc = dimethylacetamide. quant. = quantitative. n.d. = not detected.

### Catalyst deactivation causes limitations

With the optimized conditions in hand, the versatility of the semi-heterogeneous catalytic system was evaluated (Table 2). The reaction of methyl 4-bromobenzoate with cyclic secondary amines generally gave high yields for the corresponding aryl amines (**1**, **4-7**). A secondary amine with low steric hindrance also resulted in the desired aryl amine (**8**), but the majority of acyclic secondary amines did not react under these conditions (see Supplementary Figure 14). Aliphatic and aromatic primary amines reacted efficiently with methyl 4-bromobenzoate (**9-11**). A range of aryl halides containing electron-withdrawing groups coupled with high selectivity; nitriles (**12-14**), carbonyl groups (**1**, **15**, **23-24**), trifluoromethyl- (**15**) as well as methylsulfonyl-groups (**16**), halides (**17-18**), boronic acid pinacol esters (**22**),

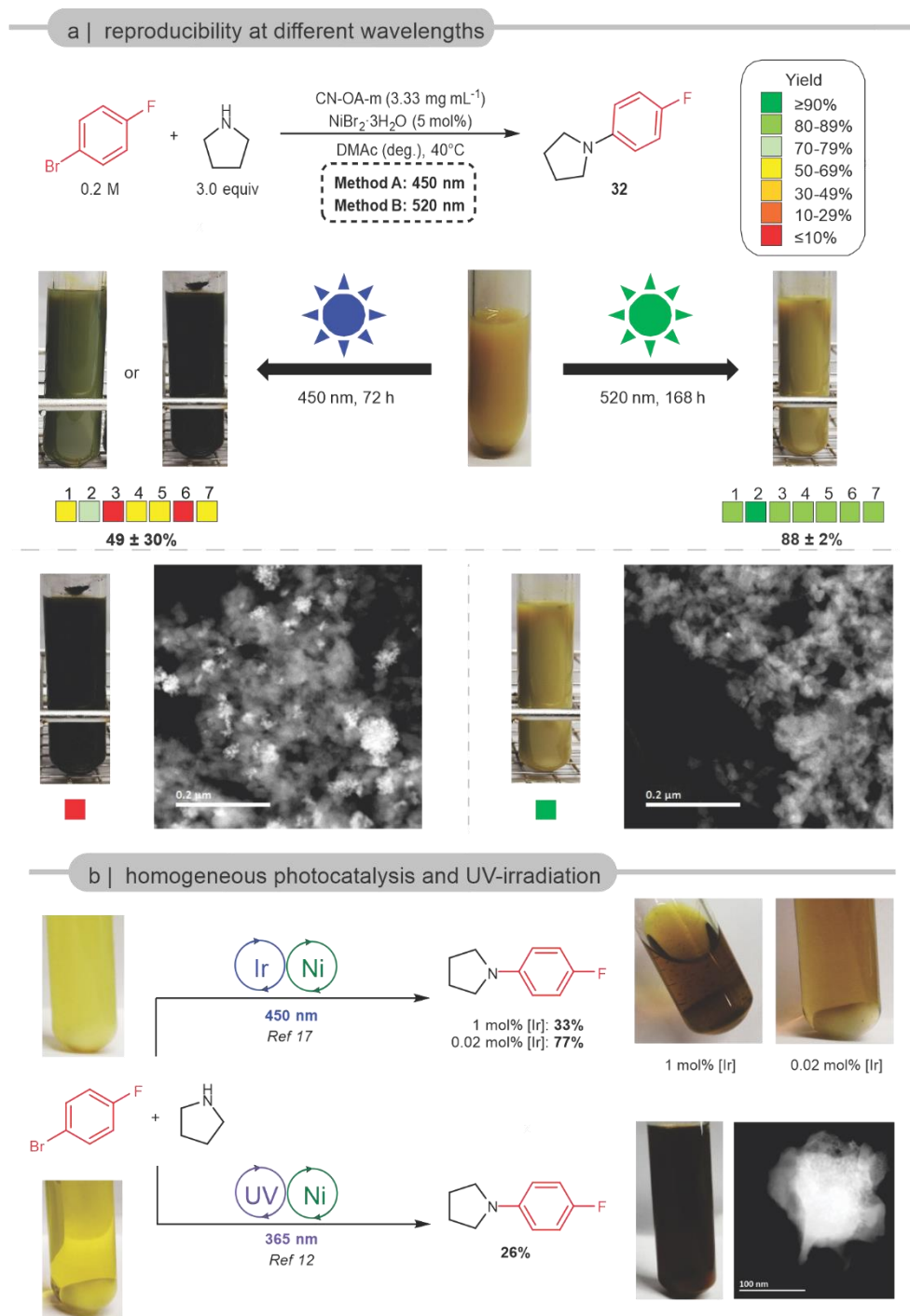
and electron-poor heteroaromatic bromides (**25**, **26**) were tolerated in the dual catalytic amination. 1,4-Dibromobenzene can undergo selective mono- (**20**) or di-amination (**21**) by varying the reaction time and stoichiometry of the amine coupling partner. Similar to related C–O bond formations,<sup>24,25</sup> a carbonyl-group in the 2-position only gave moderate yield (**16**). Low reactivity was observed for electron-rich heterocycles (**27**, **28**). Notably, good isolated yields were obtained for the C–N coupling of pyrrolidine with a range of electron-rich aryl bromides (**29–36**). Interestingly, although 2- and 3-bromoaniline (**30** & **31**) gave good yields, only a very low amount of the desired product (<5%) was formed when 4-bromoaniline was used (see Supplementary Figure 15). However, in the case of 1-bromo-4-fluorobenzene (**32**), bromobenzene (**33**), 3-bromotoluene (**34**), 1-bromo-4-*tert*-butylbenzene (**35**), and 4-bromoanisole (**36**) these values are not representative, as these substrates suffered from severe reproducibility issues. These reactions frequently resulted in low yields and the heterogeneous PRC became black, whereas almost no color change was observed in case of aryl halides that do not suffer from these reproducibility issues. High amounts of deposited nickel were detected on the recovered, black carbon nitride material by inductively coupled plasma optical emission spectrometry (ICP-OES), indicating nickel-black formation.

Table 2 | Scope of the semi-heterogeneous amination of amines and aryl bromides.<sup>[a]</sup>

## Overcoming catalyst deactivation

Deactivation of metal catalysts *via* deposition is a common problem in palladium catalysis (Pd-black formation) and can be addressed by avoiding high concentrations of Pd(0) species that

agglomerate.<sup>28</sup> In light-mediated, nickel catalysed C–N cross-couplings, a Ni(0) complex was proposed to be the catalytically active species that is initially formed *via* a photoredox-catalysed hydrogen atom transfer (HAT).<sup>20</sup> We assumed that, in the case of electron-rich aryl halides, slow oxidative addition results in the accumulation of unstabilized Ni(0) species that aggregate. Since the heterogeneous photocatalyst absorbs only weakly above 450 nm,<sup>25</sup> we assumed that the formation of nickel-black can be decelerated using higher wavelengths. As anticipated, when a mixture of pyrrolidine and CN-OA-m in DMAc was irradiated with green light (520 nm), nickel black formation was significantly slower than with blue light (450 nm, see Supplementary Note 9). To our delight, the coupling of pyrrolidine and 1-bromo-4-fluorobenzene was highly selective and reproducible using 520 nm LEDs (Method B), and the desired compound (**32**) was obtained in 85-91% in six parallel experiments (Figure 2, a; see Supplementary Note 4 for details). The same set of experiments using blue LEDs (~450 nm, Method A) exhibited large variations in yield. While five experiments gave 60-70% of **32**, only 5-6% of the desired amine were formed for two reactions where the reaction mixture turned black. Careful analysis of the heterogeneous material recovered from the low yielding reactions identified the nature and quantity of the deposited Ni species. ICP-OES analysis showed a Ni concentration of 126 mg g<sup>-1</sup> for the reaction irradiated with blue light and only 36 mg g<sup>-1</sup> for the material after an experiment using green LEDs. Elemental analysis *via* energy-dispersive X-ray spectroscopy (EDX) is in agreement with these results. X-ray powder diffraction (XRD) confirmed the deposition of low valent nickel species, with a significantly higher concentration on the material irradiated with blue light. High resolution X-ray photoelectron spectroscopy (XPS) for core levels of Ni2p<sub>3/2</sub> spectrum of the recovered CN-OA-m from experiments using 450 nm LEDs (Method A) showed two main deconvoluted peaks located at 853.7 (±0.02) eV and 852.5 (±0.02) eV that can be assigned to the binding energy of Ni(II) and Ni(0) species.



**Figure 2 | Catalyst deactivation during the reaction of 4-bromofluorobenzene with pyrrolidine.** **a**, Reproducibility using blue (450 nm) and green (520 nm) LED irradiation. The reaction mixture turned dark green or black and suffered from severe reproducibility issues at 450 nm, whereas almost no color change and reproducible results were obtained at 520 nm. HAADF-STEM images show nickel particle agglomerates (bright spots) on CN-OA-m recovered from the experiment using blue light. Almost no agglomerates are observed when a 520 nm light source was used. **c**, Nickel-black formation was also observed using the homogeneous (Ir[dF(CF<sub>3</sub>)ppy]<sub>2</sub>(dtbbpy))PF<sub>6</sub> (= [Ir]) photocatalyst and in the PRC-free reaction using UV light. DMAc = dimethylacetamide.

Only Ni(II) was detected on the material recovered from experiments using 520 nm LEDs (Method B) by XPS. Scanning transmission electron microscopy (STEM) was used to visualize nickel particles on the surface of the recovered CN-OA-m from both methods. High-angle annular dark-field (HAADF) images show a high amount of nickel particles that agglomerated (nickel-black) on the CN-OA-m recovered from experiments using 450 nm LEDs (Method A), whereas the material from experiments using 520 nm LEDs (Method B) contained almost no agglomerates (Figure 2, a).

Nickel-black formation was also shown to be responsible for low yields using other light-mediated protocols for the same model reaction (Figure 2, b; see Supplementary Note 4 for details). A reaction with 1 mol% of the homogeneous PRC (Ir[dF(CF<sub>3</sub>)ppy]<sub>2</sub>(dtbbpy))PF<sub>6</sub>,<sup>17</sup> resulted in low selectivity towards the desired coupling product (**32**, 33% yield), and small amounts of a black precipitate were formed during the reaction. Decreasing the amount of (Ir[dF(CF<sub>3</sub>)ppy]<sub>2</sub>(dtbbpy))PF<sub>6</sub> to 0.02 mol% increased the yield of **32** significantly (77%) and no particle formation was observed. Here, the amount of the PRC plays a crucial role to avoid nickel-black formation and the optimal catalyst loading needs to be determined for each substrate individually. The PRC-free, UV light-mediated protocol<sup>12</sup> resulted in no more than 26% of **32** and a black precipitate was formed in high amounts (Figure 2, c). STEM imaging and EDX spectroscopy confirmed that these solids consist of nickel and organic matter that is presumably resulting from substrate/product degradation by the high-energy light source.

The dual carbon nitride/nickel catalysed protocol using green light (520 nm, Method B) did also enable selective, reproducible C–N cross-couplings of bromobenzene (**33**), and 3-bromotoluene (**34**) with pyrrolidine, but did not eliminate catalyst deactivation issues in the cases of 1-bromo-4-*tert*-butylbenzene (**35**), and 4-bromoanisole (**36**) (Figure 3, a). Although almost quantitative product formation was observed in some cases, the reactions sometimes gave low yields and black reaction mixtures (see Supplementary Note 5 for details). In the case

of 1-bromo-4-*tert*-butylbenzene, for example, six parallel reactions using 450 nm (Method A) gave 52-70% of the desired product (**35**), whereas up to 92% as well as only 28 % were obtained under identical conditions using 520 nm (Method B). Efforts to increase the reproducibility and to minimize the nickel-black formation by changing the light intensity, distance between the reaction mixture and light source, varying the amount of both catalysts, changing the solvent or nickel catalyst, and adding MTBD (7-Methyl-1,5,7-triazabicyclo(4.4.0)dec-5-ene)<sup>17</sup> or dtbbpy to stabilize intermediate nickel species were not successful. We hypothesized that the formation of Ni(0) agglomerates can be addressed by increasing the concentration of the reaction mixture for two reasons. First, a higher concentration would increase the rate of oxidative addition, thus minimizing the accumulation of Ni(0) species. Second, catalyst deactivation might not only be accelerated by higher photon energies, but also a competitive binding of the amine and the solvent (DMAc) with low-valent nickel intermediates. In palladium catalysis, for example, PdArylXL<sub>n</sub> intermediates were reported to form complexes with various solvents, including DMAc, that undergo β-hydride elimination followed by the formation of Pd(0) and Aryl-H.<sup>29</sup> Although pyrrolidine was shown to be the primary ligand in light-mediated, nickel catalysed aminations,<sup>20</sup> the high excess of DMAc potentially results in solvent-catalyst interactions that could contribute to Ni-black formation. Indeed, running the reaction at 1.2 M instead of 0.2 M resulted in reproducible reactions and the desired products (**32-36**) were obtained in high yields, even at 450 nm (Method C). These results could not be further improved using 520 nm irradiation, suggesting that the nickel-black formation can be outpaced at high concentrations independent of the photon energy in our semi-heterogeneous catalytic system. It has to be noted that a higher concentration did not increase the yield in case of the homogenous photocatalyst (Ir[dF(CF<sub>3</sub>)ppy]<sub>2</sub>(dtbbpy))PF<sub>6</sub>.

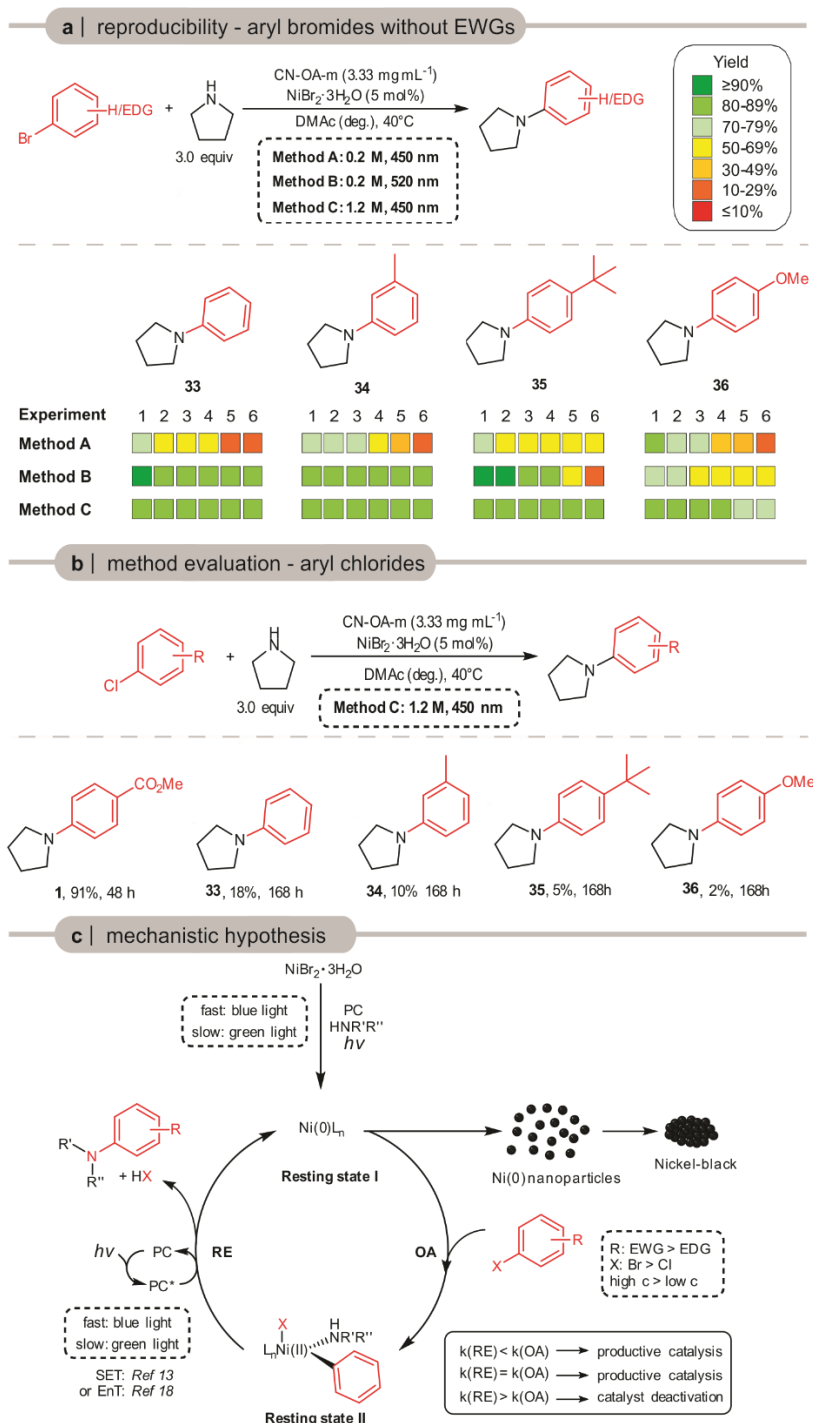


**Figure 3 | Evaluation of different coupling protocols.** **a**, Reproducibility study for aryl bromides without electron withdrawing groups using different C–N coupling protocols. NMR yields are reported **b**, Evaluation of Method C for the coupling of aryl halides and pyrrolidine. <sup>a</sup>Isolated yield. <sup>b</sup>NMR-yield **c**, Simplified mechanism of productive catalysis and catalyst deactivation. The reductive elimination (RE) likely follows either a three-step photoredox (Ni(II)-Ni(III)-Ni(I)-Ni(0));<sup>13</sup> or a two-step energy transfer (Ni(II)-Ni(II)\*-Ni(0)) process.<sup>18</sup> DMAc = dimethylacetamide. PC = photocatalyst. OA = oxidative addition. RE = reductive elimination. EWG = electron withdrawing group. EDG = electron donating group. SET = single electron transfer. EnT = energy transfer.

A reinvestigation of the coupling of methyl 4-chlorobenzoate with pyrrolidine was carried out using all protocols (see Supplementary Note 6 for details). The standard protocol (Method A) afforded the desired coupling product (**1**) in 65% within seven days. Longer irradiation did not result in higher yields and only increased the amount of the dehalogenated side product, indicating complete catalyst deactivation. With green light (Method B), 83% of **1** was obtained within 14 days. The optimized method using 450 nm LEDs and a lower amount of solvent (Method C) significantly enhanced the C–N coupling and resulted in 92% of **1** within two days (Figure 3, b). When the best conditions (Method C) were applied for electron-neutral, and -rich aryl chlorides, a clear trend was observed (Figure 3, b). Chlorobenzene gave 18% of **33** within 168 hours, and substrates with electron-donating substituents gave even lower yields. The formation of nickel black was observed in all cases.

Taking all experiments together, we propose that catalyst deactivation is avoided when the relative rate of oxidative addition (OA) is equal or higher than the relative rate of reductive elimination (RE), avoiding accumulation of Ni(0) species (Resting state I, Figure 3, c). This is (under all conditions) the case for activated (electron-poor) aryl bromides. In case of bromobenzene and 3-bromotoluene, the rate of RE (and the initial formation of Ni(0)) was sufficiently decelerated by using green light (slow OA, slow RE). At higher concentrations, the rate of OA is increased significantly, resulting in efficient productive catalysis for all tested, electron-rich aryl bromides (fast OA, fast RE). For non-activated, electron-rich aryl chlorides OA becomes too slow and Ni(0) accumulation cannot be avoided under the conditions reported herein.

### **Recycling of the heterogeneous photocatalyst**

Next, we sought to study if the deposition of nickel-black also affects the recyclability of CN-OA-m by altering its photocatalytic activity. During the coupling of pyrrolidine with methyl 4-

bromobenzoate using white (RGB) LEDs, the reaction mixture became greenish-brown (Figure 4, a). ICP-OES analysis of the heterogeneous material showed a nickel content of  $\sim 14 \text{ mg g}^{-1}$  (see Supplementary Note 7 for details). The formation of product decreased significantly when the heterogeneous PRC was recycled (Figure 4, b). When no  $\text{NiBr}_2 \cdot 3\text{H}_2\text{O}$  was added to the recovered CN-OA-m material that contains deposited nickel, only trace amounts of the C-N coupling product were observed. Further, the yellow PRC turned dark green to black and the amount of deposited Ni rose to  $\sim 61 \text{ mg g}^{-1}$  over five recycling experiments. At higher wavelengths (520 nm, Method B), the model reaction required 48 h instead of 8 h for full conversion (Figure 4, a). Although the reaction mixture did not change its color, the amount of deposited Ni was similar to the white LED experiment ( $\sim 14 \text{ mg g}^{-1}$ ). The photocatalyst did, however, not lose its catalytic activity during five recycling experiments and was recovered as a yellow solid that contained a lower amount of deposited nickel ( $\sim 39 \text{ mg g}^{-1}$ ) compared to the white light experiment (Figure 4, b). Scanning transmission electron microscopy (STEM) of CN-OA-m from both recycling studies showed a significant amount of nickel agglomerates (nickel-black) for CN-OA-m from the experiments using white LEDs, whereas almost no agglomerates were detected on the semiconductor recovered from the recycling study using green LEDs.

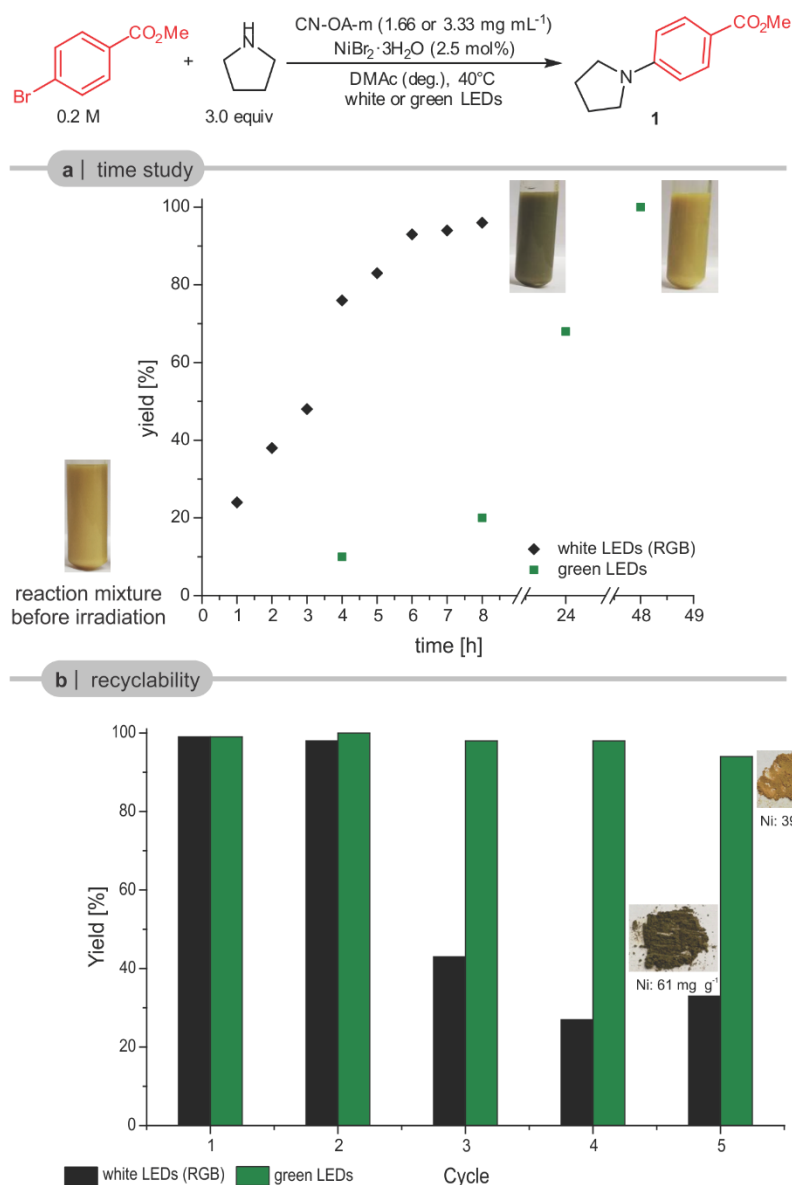


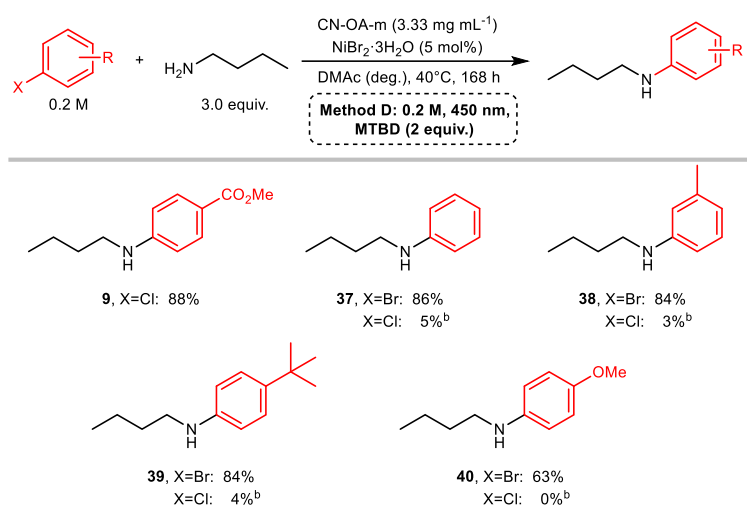
**Figure 4 | Reduction of catalyst deactivation using higher wavelengths.** **a**, Time study for the coupling of methyl 4-bromobenzoate and pyrrolidine using white (RGB) and green (~520 nm) LED irradiation. The heterogeneous photocatalyst turned green using white light (RGB) irradiation whereas no color change was observed when green light (~520 nm) was used. **b**, The recyclability of CN-OA-m is excellent using green (~520 nm) LEDs. Deactivation of the PRC by nickel-black depositions was observed using white (RGB) LEDs.

### Overcoming catalyst deactivation for primary amines

Finally, we sought to determine if deactivation of the nickel catalyst could also be avoided when less nucleophilic, primary amines are used. These substrates are usually less efficient and give lower yields than cyclic, secondary amines, even with electron-deficient aryl bromides.<sup>12,13,18,19,27</sup> By studying the cross-coupling of *n*-butylamine with 1-bromo-4-*tert*-

butylbenzene, we observed only 8% of the desired product (**39**) during a 16 h experiment using blue light (Method A, see Supplementary Note 8 for details). Notably, running the reaction at higher concentrations decreased the yield, indicating that low-valent Ni(*n*-butylamine)<sub>n</sub> species are rather inefficient towards OA and a higher concentration in this case might even accelerate catalyst deactivation. Increasing the temperature from 40 to 60 °C resulted in up to 42% of the desired coupling product (**39**), but concomitant deactivation of the nickel catalyst was observed. Switching to green light or performing the reaction at 80 °C did not improve these results.

The above described strategies to accelerate OA or decelerate RE were not successful. It was previously reported that the addition of DBU and MTBD has a positive effect on the reaction outcome with primary amines, but the reason for that remains unclear.<sup>15,17</sup> We assumed that coordination of these additives to the active, low valent nickel species might activate the low-valent nickel complex towards OA, and has a stabilizing effect that would increase the lifetime of resting state **I** by inhibiting nickel-black formation. We could ultimately prove this stabilizing affect during control experiments in the absence of aryl halides (see Supplementary Note 9). When NiBr<sub>2</sub>·3H<sub>2</sub>O was irradiated in the presence of pyrrolidine with blue light, Ni-black was rapidly formed. However, the formation of nickel black took significantly longer in the presence of MTBD. Further, a comparison of the coupling of 1-bromo-4-*tert*-butylbenzene with *n*-butylamine with and without additives showed a higher catalytic activity when MTBD was added. After a short optimization, we obtained conditions that enabled the coupling of electron-poor aryl bromides with *n*-butylamine in good to excellent selectivity at 40°C (Table 3). This method was also applicable for an electron-poor aryl chloride, but, similar to the coupling with pyrrolidine, deactivated aryl chlorides remain a limitation.

Table 3 | Semi-heterogeneous amination of primary amines and aryl halides.<sup>[a]</sup>

<sup>a</sup>Reaction conditions: aryl halide (1.2 mmol), *n*-butylamine (3.6 mmol), CN-OA-m (20 mg), NiBr<sub>2</sub>·3H<sub>2</sub>O (60 μmol), MTBD (2.4 mmol), DMac (anhydrous, 6.0 mL), blue LEDs at 40 °C. Isolated yields are reported. <sup>b</sup>Yield was determined by <sup>1</sup>H-NMR using 1,3,5-trimethoxybenzene as internal standard. DMac = dimethylacetamide. MTBD = 7-Methyl-1,5,7-triazabicyclo[4.4.0]dec-5-ene.

## Conclusion

The formation of nickel-black limits the applicability of light-mediated, nickel catalysed C–N cross-couplings. In particular, aryl bromides lacking electron-withdrawing groups suffer from reproducibility problems due to deactivation of the nickel catalyst. Deposition of nickel particles (nickel-black) not only deactivates the homogeneous nickel catalyst, but also the heterogeneous carbon nitride photocatalyst. Careful studies using dual carbon nitride/nickel catalysis showed that nickel-black formation likely results from a slow oxidative addition in case of electron-rich aryl bromides, leading to accumulation of low-valent nickel species that agglomerate. We showed that this issue can be overcome by decreasing the rate of the reductive elimination, increasing the rate of oxidative addition, and stabilizing low-valent nickel intermediates with a suitable additive. Our strategies enable reproducible, highly selective C–N cross-couplings of electron-rich, -neutral and -poor aryl bromides with primary and cyclic, secondary amines and can even be used for efficient reactions of electron-poor aryl chlorides.

## Methods

**General remarks.** Substrates, reagents, and solvents were purchased from commercial suppliers and used without further purification.  $^1\text{H}$ -,  $^{13}\text{C}$ - and  $^{19}\text{F}$ -NMR spectra were obtained using a Varian 400 spectrometer (400 MHz, Agilent), an Ascend<sup>TM</sup> 400 spectrometer (400 MHz, cryoprobe, Bruker) and a Varian 600 spectrometer (600 MHz, Agilent) at 298 K, and are reported in ppm relative to the residual solvent peaks. Peaks are reported as: s = singlet, d = doublet, t = triplet, q = quartet, m = multiplet or unresolved, with coupling constants in Hz. Analytical thin layer chromatography (TLC) was performed on pre-coated TLC-sheets, ALUGRAM Xtra SIL G/UV<sub>254</sub> sheets (Macherey-Nagel) and visualized with 254 nm light or staining solutions followed by heating. Purification of final compounds was carried out by flash chromatography on the Reveleris X2 Flash Chromatography System from GRACE using prepacked columns with 40  $\mu\text{m}$  silica gel. Silica 60 M (0.04-0.063 mm) silica gel (Sigma Aldrich) was used for dry loading of the crude compounds on the flash chromatography system. Centrifugation was carried out using an Eppendorf 5430 centrifuge. High-resolution mass spectral data were obtained using a HR-EI-MS (Waters Autospec Premier) and a Waters XEVO G2-XS 4K spectrometer with the XEVO G2-XS QTOF capability kit. Emission spectra of LED lamps were recorded using 10 in. (24.5 cm) integrating sphere (Labsphere, Inc. Model LMS 1050) equipped with a diode array detector (International Light, Model RPS900). The UV/Vis spectrum of  $\text{Ir}(\text{ppy})_2(\text{dtbbpy})\text{PF}_6$  was recorded using a UVmini-1240 spectrometer (Shimadzu). Inductively coupled plasma - optical emission spectrometry (ICP-OES) was carried out using a Horiba Ultra 2 instrument equipped with photomultiplier tube detection. FTIR spectra were recorded on a Thermo Scientific Nicolet iD5 spectrometer. Diffuse reflectance UV/Vis spectra of powders were recorded on a Shimadzu UV-2600 spectrometer equipped with an integrating sphere. For XRD measurements, a Bruker D8 Advanced X-ray diffractometer with  $\text{Cu K}\alpha$  radiation was used. Scanning electron microscopy (SEM) images were obtained on a LEO 1550-Gemini microscope. Energy-dispersive X-ray (EDX) investigations were conducted on a

Link ISIS-300 system (Oxford Microanalysis Group) equipped with a Si(Li) detector and an energy resolution of 133 eV. X-ray photoelectron spectroscopic (XPS) measurements were carried out with a CISSY set-up, equipped with a SPECS XR 50 X-ray gun with Mg K $\alpha$  excitation radiation (1254.6 eV) and combined with a lens analyzer module (CLAM) under ultra-high vacuum (UHV,  $1.5 \times 10^{-8}$  Pa). The calibration was performed using the Au 4f $_{7/2}$  (84.0 eV) binding energy scale as reference. Quantitative analysis and deconvolution were achieved using “peakfit” and “Igor” software with Lorentzian-Gaussian functions and Shirley background deletion in photoemission spectra. The STEM images were acquired using a double-corrected Jeol ARM200F, equipped with a cold field emission gun. For the investigation, the acceleration voltage was set to 200 kV, the emission was put to 5  $\mu$ A and a condenser aperture with a diameter of 20  $\mu$ m was used. With these settings, the microscope reaches a lattice resolution below 1 Å. The STEM specimens were prepared by dissolving a powder sample of the material in ethanol, sonicating the solution for 15 minutes and finally dropping a few drops onto a copper TEM grid coated with holey carbon film. Once the solution had dried off, the specimens were investigated.

**Preparation of the heterogeneous photocatalyst.** The synthesis of CN-OA-m was carried out using a slightly adapted version of the literature procedure:<sup>30</sup> For each batch of the photocatalyst, urea (10 g, 166.5 mmol) and oxamide (0.5 g, 5.7 mmol) were mixed in 10 ml of DI water to generate a homogeneous mixture. After drying at 373 K, the resulting solids were grinded, transferred into a crucible with a cover and heated up in an air-oven with a heating rate of 4.3 K/min to 773 K. After keeping the mixture for 2h at 773 K, the sample was allowed to cool to room temperature. Subsequently, KCl (3.3 g, 44.3 mmol) and LiCl (2.7 g, 63.7 mmol) were added and the solids were grinded to obtain a homogeneous mixture which was heated in an inert atmosphere (N $_2$  flow: 5 mL/min) to 823 K with a heating rate of 4.6 K/min. After

keeping the mixture for 2 h at 823 K, the sample was allowed to cool to room temperature and the resulting solids were collected on a filter paper and washed with H<sub>2</sub>O (3 x 100 mL). The resulting yellow material was dried at 373 K (average yield per batch: ~425 mg). All analytical data (FTIR, UV/Vis, XRD, SEM, etc.) are in full agreement with those published in the literature.<sup>30</sup>

**Setup for photochemical reactions.** A flexible, red/green/blue LED strip (RGB, 5m, 24 W/strip; for details see Supplementary Figure 11) was wrapped around a 115 mm borosilicate crystallization dish. Blue, green, red or white (illumination of all three LED colors - red/green/blue) light was used at full power for all experiments (For emission spectra of a single diode, see Supplementary Figure 12). The evaporating dish was filled with ethylene glycol and the temperature was set to 40°C to maintain a constant temperature. The sealed, cylindrical reaction vessels (16 x 100 mm) were placed at the same distance from the LED strip during all experiments. All reactions were performed with a stirring speed of 600 (1 mL) or 1400 rpm (3 or 6 mL). For large scale aminations a flexible, red/green/blue LED strip (RGB, 5m, 24 W/strip) was wrapped around a 115mm borosilicate beaker (for details see Supplementary Figure 11). The scale-up reaction was performed in a sealed, cylindrical reaction vessel (25 x 140 mm) with a stirring speed of 700 rpm and without additional heating.

**General procedure for light-mediated C–N cross-couplings using CN-OA-m and Ni catalysis.** An oven dried vial (19 x 80 mm) equipped with a stir bar was charged with CN-OA-m (20 mg), aryl bromide (1.2 mmol, 1.0 equiv.) and NiBr<sub>2</sub>·3H<sub>2</sub>O (2.5-5.0 mol%). Subsequently, the amine (3.6 mmol, 3.0 equiv.) 7-Methyl-1,5,7-triazabicyclo[4.4.0]dec-5-ene (MTBD, only required for Method D) (367.8 mg, 344.7 µl, 2.4 mmol, 2.0 equiv.) and DMAc (anhydrous, Method A, B, and D: 6 mL, Method C: 1 mL) were added and the vial was sealed

with a septum and Parafilm. The reaction mixture was sonicated for 5-10 min until fine dispersion of the solids was achieved and the mixture was then degassed by bubbling N<sub>2</sub> for 10 min. The mixture was irradiated in the photoreactor (Method A, C and D: 450 nm, Method B: 520 nm) at 40 °C. After the respective reaction time, one equivalent of 1,3,5-trimethoxybenzene (202.0 mg, 1.2 mmol, internal standard) was added. An aliquot (~300 µL) of the reaction mixture was diluted with DMSO-d<sub>6</sub> and subjected to <sup>1</sup>H-NMR analysis. After full consumption of the arene starting material, the liquid phase was diluted with H<sub>2</sub>O (40 mL) and extracted with ethyl acetate (3 x 30 mL). The combined organic phases were washed with H<sub>2</sub>O (40 mL), NaHCO<sub>3</sub> solution (40 ml) and brine (40 mL), dried over Na<sub>2</sub>SO<sub>4</sub> and concentrated. The crude product was purified by flash column chromatography (SiO<sub>2</sub>, Hexane/EtOAc, dichloromethane/EtOAc or dichloromethane/MeOH) on a Grace™ Reveleris™ system using a 12 g cartridge to afford the desired product. The final product was characterized by <sup>1</sup>H-NMR, <sup>13</sup>C-NMR, <sup>19</sup>F-NMR and HRMS.

**Recycling studies.** An oven dried vial (13 x 80 mm) equipped with a stir bar was charged with CN-OA-m (20 mg), methyl 4-bromobenzoate (258.0 mg, 1.2 mmol, 1.0 equiv.) and NiBr<sub>2</sub>·3H<sub>2</sub>O (8.2 mg, 30 µmol, 2.5 mol%). Subsequently, pyrrolidine (256.0 mg, 295.6 µl, 3.6 mmol, 3.0 equiv.) and DMAc (anhydrous, 6 mL) were added and the vial was sealed with a septum and Parafilm. The reaction mixture was sonicated for 5-10 min followed by stirring for 5 min until fine dispersion of the solids was achieved and the mixture was then degassed by bubbling N<sub>2</sub> for 10 min. The mixture was irradiated in the photoreactor (white light or green light) at 40 °C with rapid stirring (1400 rpm). After the respective reaction time, one equivalent of 1,3,5-trimethoxybenzene (202.0 mg, 1.2 mmol) was added and the mixture was stirred for 5 min. The reaction mixture was centrifuged at 3000 rpm for 20 min and the liquid phase was carefully separated and analyzed by <sup>1</sup>H-NMR. The carbon nitride was washed with DMAc

(anhydrous, 6 mL, followed by centrifugation at 3000 rpm for 20 min and separation of the liquid phase), lyophilized (overnight) and reused in the next reaction.

### Data availability

Experimental procedures, and relevant material and compound characterization data are available in the Supplementary Information. Any other data is available from the authors on reasonable request.

### References

- 1 Roughley, S. D. & Jordan, A. M. The Medicinal Chemist's Toolbox: An Analysis of Reactions Used in the Pursuit of Drug Candidates. *J. Med. Chem.* **54**, 3451-3479, (2011).
- 2 Wolfe, J. P. & Buchwald, S. L. Nickel-Catalyzed Amination of Aryl Chlorides. *J. Am. Chem. Soc.* **119**, 6054-6058, (1997).
- 3 Ge, S., Green, R. A. & Hartwig, J. F. Controlling First-Row Catalysts: Amination of Aryl and Heteroaryl Chlorides and Bromides with Primary Aliphatic Amines Catalyzed by a BINAP-Ligated Single-Component Ni(0) Complex. *J. Am. Chem. Soc.* **136**, 1617-1627, (2014).
- 4 Tassone, J. P., England, E. V., MacQueen, P. M., Ferguson, M. J. & Stradiotto, M. PhPAd-DalPhos: Ligand-Enabled, Nickel-Catalyzed Cross-Coupling of (Hetero)aryl Electrophiles with Bulky Primary Alkylamines. *Angew. Chem.; Int. Ed.* **58**, 2485-2489, (2019).
- 5 Kelly, R. A., Scott, N. M., Díez-González, S., Stevens, E. D. & Nolan, S. P. Simple Synthesis of CpNi(NHC)Cl Complexes (Cp = Cyclopentadienyl; NHC = N-Heterocyclic Carbene). *Organometallics* **24**, 3442-3447, (2005).
- 6 Park, N. H., Teverovskiy, G. & Buchwald, S. L. Development of an Air-Stable Nickel Precatalyst for the Amination of Aryl Chlorides, Sulfamates, Mesylates, and Triflates. *Org. Lett.* **16**, 220-223, (2014).

- 7 Kampmann, S. S., Skelton, B. W., Wild, D. A., Koutsantonis, G. A. & Stewart, S. G. An Air-Stable Nickel(0) Phosphite Precatalyst for Primary Alkylamine C–N Cross-Coupling Reactions. *Eur. J. Org. Chem.* **2015**, 5995-6004, (2015).
- 8 Shields, J. D., Gray, E. E. & Doyle, A. G. A Modular, Air-Stable Nickel Precatalyst. *Org. Lett.* **17**, 2166-2169, (2015).
- 9 McGuire, R. T., Paffile, J. F. J., Zhou, Y. & Stradiotto, M. Nickel-Catalyzed C–N Cross-Coupling of Ammonia, (Hetero)anilines, and Indoles with Activated (Hetero)aryl Chlorides Enabled by Ligand Design. *ACS Catal.* **9**, 9292-9297, (2019).
- 10 Li, C. *et al.* Electrochemically Enabled, Nickel-Catalyzed Amination. *Angew. Chem.; Int. Ed.* **56**, 13088-13093, (2017).
- 11 Kawamata, Y. *et al.* Electrochemically Driven, Ni-Catalyzed Aryl Amination: Scope, Mechanism, and Applications. *J. Am. Chem. Soc.* **141**, 6392-6402, (2019).
- 12 Lim, C.-H., Kudisch, M., Liu, B. & Miyake, G. M. C–N Cross-Coupling via Photoexcitation of Nickel–Amine Complexes. *J. Am. Chem. Soc.* **140**, 7667-7673, (2018).
- 13 Du, Y. *et al.* Strongly Reducing, Visible-Light Organic Photoredox Catalysts as Sustainable Alternatives to Precious Metals. *Chem. Eur. J.* **23**, 10962-10968, (2017).
- 14 Caputo, J. A. *et al.* General and Efficient C–C Bond Forming Photoredox Catalysis with Semiconductor Quantum Dots. *J. Am. Chem. Soc.* **139**, 4250-4253, (2017).
- 15 Liu, Y.-Y., Liang, D., Lu, L.-Q. & Xiao, W.-J. Practical heterogeneous photoredox/nickel dual catalysis for C–N and C–O coupling reactions. *Chem. Commun.* **55**, 4853-4856, (2019).
- 16 Ghosh, I. *et al.* Organic semiconductor photocatalyst can bifunctionalize arenes and heteroarenes. *Science* **365**, 360-366, (2019).
- 17 Corcoran, E. B. *et al.* Aryl amination using ligand-free Ni(II) salts and photoredox catalysis. *Science* **353**, 279-283, (2016).
- 18 Escobar, R. A. & Johannes, J. A Unified and Practical Method for Carbon-Heteroatom Cross-Coupling via Nickel/Photo Dual Catalysis. *Chem. Eur. J.*, accepted article, <https://doi.org/10.1002/chem.202000052>.

- 19 Kudisch, M., Lim, C.-H., Thordarson, P. & Miyake, G. M. Energy Transfer to Ni-amine Complexes in Dual Catalytic, Light-driven C–N Cross-Coupling Reactions. *J. Am. Chem. Soc.* **141**, 19479-19486, (2019).
- 20 Qi, Z.-H. & Ma, J. Dual Role of a Photocatalyst: Generation of Ni(0) Catalyst and Promotion of Catalytic C–N Bond Formation. *ACS Catal.* **8**, 1456-1463, (2018).
- 21 Wang, C., Cao, S. & Fu, W.-F. A stable dual-functional system of visible-light-driven Ni(ii) reduction to a nickel nanoparticle catalyst and robust in situ hydrogen production. *Chem. Commun.* **49**, 11251-11253, (2013).
- 22 Rodríguez, J. L., Valenzuela, M. A., Pola, F., Tiznado, H. & Poznyak, T. Photodeposition of Ni nanoparticles on TiO<sub>2</sub> and their application in the catalytic ozonation of 2,4-dichlorophenoxyacetic acid. *J. Mol. Catal. A Chem.* **353-354**, 29-36, (2012).
- 23 Indra, A. *et al.* Nickel as a co-catalyst for photocatalytic hydrogen evolution on graphitic-carbon nitride (sg-CN): what is the nature of the active species? *Chem. Commun.* **52**, 104-107, (2016).
- 24 Cavedon, C., Madani, A., Seeberger, P. H. & Pieber, B. Semiheterogeneous Dual Nickel/Photocatalytic (Thio)etherification Using Carbon Nitrides. *Org. Lett.* **21**, 5331-5334, (2019).
- 25 Pieber, B. *et al.* Semi-Heterogeneous Dual Nickel/Photo-catalysis using Carbon Nitrides: Esterification of Carboxylic Acids with Aryl Halides. *Angew. Chem. Int. Ed.* **58**, 9575-9580 (2019).
- 26 Zhang, G. *et al.* Optimizing Optical Absorption, Exciton Dissociation, and Charge Transfer of a Polymeric Carbon Nitride with Ultrahigh Solar Hydrogen Production Activity. *Angew. Chem.; Int. Ed.* **56**, 13445-13449, (2017).
- 27 Rosso, C. *et al.* An oscillatory plug flow photoreactor facilitates semi-heterogeneous dual nickel/carbon nitride photocatalytic C–N couplings. *React. Chem. Eng.* **5**, 597-604, (2020).
- 28 Crabtree, R. H. Deactivation in Homogeneous Transition Metal Catalysis: Causes, Avoidance, and Cure. *Chem. Rev.* **115**, 127-150, (2015).

- 29 Molina de la Torre, J. A., Espinet, P. & Albéniz, A. C. Solvent-Induced Reduction of Palladium-Aryls, a Potential Interference in Pd Catalysis. *Organometallics* **32**, 5428-5434, (2013).
- 30 Zhang, G. *et al.* *Angew. Chem. Int. Ed.* **56**, 13445-13449, (2017).

### **Acknowledgments**

We gratefully acknowledge the Max-Planck Society for generous financial support. S.G. and B.P. thank the International Max Planck Research School on Multiscale Bio-Systems for funding. B.P. and S.R. acknowledge financial support by a Liebig Fellowship of the German Chemical Industry Fund (Fonds der Chemischen Industrie, FCI). B.P. thanks the Deutsche Forschungsgemeinschaft (DFG, German Research Foundation) under Germany's Excellence Strategy – EXC 2008 – 390540038 – UniSysCat for financial support. We thank our colleagues Prof. Peter H. Seeberger, Dr. Jamal Malik, Dr. Kerry Gilmore, Dr. Tobias Heil, Dr. Daniel Cruz, Heike Runge, Rona Pitschke, Jessica Brandt and Katharina ten Brummelhuis (all MPIKG), for scientific, technical and analytical support.

### **Author contributions**

B.P. conceived and directed the research study. B.P., S.G. and S.R. designed all experiments. S.G. performed all synthetic experiment. S.G. and S.R. carried out characterizations of materials and studies on the Ni-black formation. S.G. and B.P. wrote the manuscript with contributions from S.R.

### **Competing interest**

The authors declare no competing interests.